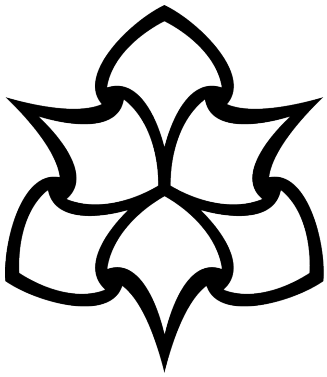

Atmospheric Environment 95 (2014) 468–479

Contents lists available at ScienceDirect

Atmospheric Environment

journal homepage: www.elsevier.com/locate/atmosenv

Aircraft emission mitigation by changing route altitude: A multi-model estimate of aircraft NO_x emission impact on O_3 photochemistry

Ole Amund Søvde [a, *], Sigrun Matthes [b], Agnieszka Skowron [c], Daniela Iachetti [d], Ling Lim [c], Bethan Owen [c], Øivind Hodnebrog [a], Glauco Di Genova [d], Gianni Pitari [d], David S. Lee [c], Gunnar Myhre [a], Ivar S.A. Isaksen [a, e]

[a] Center for International Climate and Environmental Research – Oslo (CICERO), Oslo, Norway
[b] Deutsches Zentrum für Luft- und Raumfahrt, Institut für Physik der Atmosphäre, Oberpfaffenhofen, Germany
[c] Dalton Research Institute, Manchester Metropolitan University, Manchester, United Kingdom
[d] University of L'Aquila, L'Aquila, Italy
[e] Department of Geosciences, University of Oslo, Oslo, Norway

HIGHLIGHTS

- Multi-model study on the aircraft NOx-related effect on the atmosphere.
- New inventory for aircraft NO_x emissions, representative for year 2006.
- The total RF due to NO_x emissions is found to be about 5 mW m^2.
- Shifting cruise altitudes up or down by 2000 ft changes RF by about 2 mW m^2.
- Contrail-avoiding measures will likely give small NO_x impact.

GRAPHICAL ABSTRACT

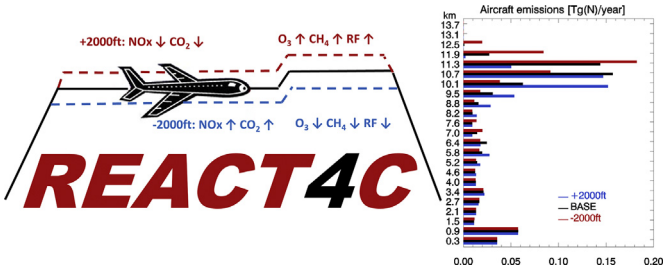

ARTICLE INFO

Article history:
Received 10 February 2014
Received in revised form
19 June 2014
Accepted 23 June 2014
Available online 24 June 2014

Keywords:
Aircraft NO_x emissions
Chemical impact
Radiative forcing
Multimodel comparison
Contrail avoiding measures

ABSTRACT

The atmospheric impact of aircraft NO_x emissions are studied using updated aircraft inventories for the year 2006, in order to estimate the photochemistry-related mitigation potential of shifting cruise altitudes higher or lower by 2000 ft. Applying three chemistry-transport models (CTM) and two climate-chemistry models (CCM) in CTM mode, all including detailed tropospheric and stratospheric chemistry, we estimate the short-lived radiative forcing (RF) from O_3 to range between 16.4 and 23.5 mW m^{-2}, with a mean value of 19.5 mW m^{-2}. Including the long-lived RF caused by changes in CH_4, the total NO_x-related RF is estimated to about 5 mW m^{-2}, ranging 1–8 mW m^{-2}. Cruising at 2000 ft higher altitude increases the total RF due to aircraft NO_x emissions by 2 ± 1 mW m^{-2}, while cruising at 2000 ft lower altitude reduces RF by 2 ± 1 mW m^{-2}. This change is mainly controlled by short-lived O_3 and show that chemical NO_x impact of contrail avoiding measures is likely small.

1. Introduction

In this multi-model study we assess how conceptual changes to aircraft flight altitude can alter the impact of aircraft NO_x emissions on atmospheric gas phase chemistry. Aircraft NO_x emissions have

* Corresponding author.
E-mail address: asovde@cicero.oslo.no (O.A. Søvde).

http://dx.doi.org/10.1016/j.atmosenv.2014.06.049

long been known to affect atmospheric O_3 (e.g. Johnston, 1971; Hesstvedt, 1974; Hidalgo and Crutzen, 1977), and research on the radiative impacts of aircraft emissions were recently summarised by Lee et al. (2010), later to be revisited by Myhre et al. (2011). Aircraft engines produce different types of exhaust gases and particles. Of gases, NO_x and H_2O are most important for the reactive gas phase chemistry, affecting O_3 production and loss through the O_3–NO_x chemistry (Johnston, 1971; Hidalgo and Crutzen, 1977; Johnson et al., 1992; Schumann, 1997; Dameris et al., 1998; Grewe et al., 2002; Gauss et al., 2006). Emitted particles may affect the atmospheric composition by providing surfaces for heterogeneous reactions (e.g. Lee et al., 2010). Aircraft emissions also produce contrail cirrus (e.g. Burkhardt and Kärcher, 2011; Yi et al., 2012) and CO_2. Such changes will affect the radiative balance, imposing a radiative forcing (RF). However, our focus is on reactive gas-phase chemistry only, more specifically on the effect of NO_x emissions from aircraft.

The atmospheric impact of emissions of short-lived gases have in general been found to depend strongly on where they are emitted (Berntsen et al., 2006), including aircraft NO_x emissions (Stevenson and Derwent, 2009; Köhler et al., 2013), in compliance with earlier work showing that radiative forcing from O_3 is strongest in the upper troposphere and lower stratosphere (UTLS) due to low temperatures and clean background atmosphere (e.g. Wang and Sze, 1980; Lacis et al., 1990; Hansen et al., 1997; Forster and Shine, 1997). Could relatively simple mitigation strategies for aircraft emissions reduce the atmospheric impact? In light of this question, we assess here two mitigation options using idealised emission inventories in sophisticated chemistry-transport models (CTM).

During the EU project Reducing Emissions from Aviation by Changing Trajectories for the benefit of Climate (REACT4C), three sets of aircraft emission inventories were produced, to assess the NO_x impact of shifting aircraft cruise altitudes by one flight level, i.e. representative for typical contrail-avoiding measures.

Related studies were carried out in the project TradeOff (Gauss et al., 2006; Stordal et al., 2006), and recently Frömming et al. (2012) re-investigated TradeOff inventories. Related studies have also been carried out for a possible future stratospheric fleet (Grewe et al., 2007; Pitari et al., 2008; Søvde et al., 2007). Here, we use 3 CTMs and 2 climate-chemistry models (CCM) run in CTM mode. Important improvements from previous studies are the multi-model approach, update to more recent aircraft traffic inventories, increased model resolution, and that all models comprise detailed chemistry in the troposphere and the stratosphere, fully covering the UTLS where most aircraft have their cruise altitude and hence main emissions.

The models are described in Section 2, and the aircraft emission inventories in Section 3. Atmospheric impacts are presented in Section 4 and the changes in RF in Section 5. We summarise the study in Section 6.

2. The models

Five different models are used in this study; MOZART-3, ULAQ-CTM, EMAC QCTM, Oslo CTM2 and Oslo CTM3. A short description of the models and their basic set-ups are presented next. In Supplementary Material (SM) Sect. S1, a model overview table is presented and additional information on annual emission numbers is given. We note that our models are spun up for at least 4 years, which we have found sufficient for this study. Except for ULAQ-CTM, the models are driven by or nudged to real meteorology from the European Centre for Medium-Range Weather Forecasts (ECMWF), as will be explained.

2.1. MOZART-3 CTM

The Model for OZone and Related Tracers, version 3 (MOZART-3) is a three dimensional CTM, comprehensively evaluated by Kinnison et al. (2007) and extensively used for different application studies (Gettelman et al., 2004; Park et al., 2004; Sassi et al., 2004; Liu et al., 2009; Wuebbles et al., 2011; Skowron et al., 2013). The horizontal resolution is T42 ($\approx 2.8^\circ \times 2.8^\circ$) and the vertical domain extends from surface to 0.1 hPa with 60 hybrid layers. Vertical resolution is 700–900 m at aircraft cruise altitudes (250–200 hPa). The transport of chemical compounds as well as hydrological cycle is driven by the meteorological fields from ECMWF Interim 6-h reanalysis (ERA-Interim).

MOZART-3 is built on the framework of the transport model MATCH (Model for Atmospheric Transport and Chemistry, Rasch et al., 1997) and accounts for advection, convection, boundary layer exchanges and wet removal and dry deposition. Advection of tracers is performed following the numerically fast flux-form semi-Lagrangian scheme of Lin and Rood (1996). Convective mass fluxes are re-diagnosed by MATCH, using the shallow and mid-level convection scheme of Hack (1994) and deep convective transport formulation of Zhang and McFarlane (1995).

MOZART-3 represents detailed chemical and physical processes in the troposphere and the stratosphere. The chemical mechanism consists of 108 species, 218 gas-phase reactions and 71 photolytic reactions including the photochemical reactions associated with organic halogen compounds. The species included within this mechanism are members of the O_x, NO_x, HO_x, ClO_x and BrO_x chemical families, along with CH_4 and its degradation products. A non-methane hydrocarbon oxidation scheme is also represented. The kinetic and photochemical data are from Sander et al. (2006).

The anthropogenic (non-aviation) and biomass burning surface emissions are taken from Lamarque et al. (2010), while the biogenic surface emissions are taken from POET (Granier et al., 2005). All surface emissions represent year 2000. NO_x emissions from lightning are distributed according to the location of the convective clouds based on Price et al. (1997) with a vertical profile following Pickering et al. (1998).

2.2. EMAC QCTM

The EMAC QCTM is the global ECHAM/MESSy Atmospheric Chemistry (EMAC) run in a quasi-CTM mode. EMAC is a numerical chemistry and climate simulation system that includes submodels describing tropospheric and middle atmosphere processes and their interaction with oceans, land and human influences (Jöckel et al., 2010). It uses the second version of the Modular Earth Submodel System (MESSy2, Jöckel et al., 2010). The core atmospheric model is the 5th generation European Centre Hamburg general circulation model (ECHAM5, Roeckner et al., 2003, 2006). Free troposphere dynamics (up to about 200 hPa) are nudged towards the analysed ECMWF meteorology, and in this study aviation emission interact only on chemical processes, and not with model dynamics (Deckert et al., 2011). A horizontal resolution of T42 with 90 vertical hybrid pressure levels up to 0.01 hPa is used. Vertical resolution is ~660 m at aircraft cruise altitudes.

This results in realistic atmospheric dynamics, and clouds are treated in a standard EMAC scheme (Sundqvist, 1978; Lohmann and Roeckner, 1996). An aerosol climatology (Tanré et al., 1984) is used for the calculation of the radiation field and separate climatologies are used in the troposphere (Kerkweg, 2005) and stratosphere for H_2SO_4 (Stratospheric Aerosol and Gas Experiment – SAGE) to provide aerosol surfaces for heterogeneous chemistry. Gas phase chemistry is calculated with the MECCA1 chemistry submodel (Sander et al., 2005) consistently from the surface to the

stratosphere. The applied chemical mechanism includes full stratospheric complexity, but neglects the sulphur and halogen families in the troposphere. It has been evaluated by Jöckel et al. (2006).

Anthropogenic emissions are taken from Lamarque et al. (2010), while biomass burning is from GFEDv3.1. Biomass burning is distributed in one level only (140 m thick). Lightning NO_x is distributed horizontally following Grewe et al. (2001), and vertically following Pickering et al. (1998). A base value of 5 Tg (N) yr^{-1} is applied, for which the meteorological conditions may impose a 5–10% variation on annual basis. Total emissions are listed in SM Sect. S1, where surface NO_x also includes a soil source. Other emissions depending on meteorological conditions are the soil source with a base value of 7 Tg (N) yr^{-1}, and the isoprene emissions having a base value of 315 Tg (C) yr^{-1}. Also for these the annual variation caused by meteorology is 5–10%.

2.3. ULAQ-CTM

The University of L'Aquila model is a global scale climate-chemistry coupled model (ULAQ-CCM, Pitari et al., 2002; Eyring et al., 2006; Morgenstern et al., 2010) extending from the surface to the mesosphere (0.04 hPa) and operated here in CTM mode. Dynamical data, i.e. velocity stream-function and velocity potential, are provided by the background GCM run in a reference case, with no feedbacks of aviation induced changes. Horizontally, a T21 spectral resolution is used in a $6^\circ \times 5^\circ$ grid. Vertically the model spans 126 log-pressure levels (~560 m spacing).

The ULAQ-CCM has been fully described in Pitari et al. (2002) and also in Eyring et al. (2006) and Morgenstern et al. (2010) for the SPARC-CCMVal model inter-comparison and validation campaigns. Since then, some important updates have been made in the model: (a) increase of horizontal and vertical resolution to T21 and 126 layers as described above; (b) inclusion of a numerical code for the formation of upper tropospheric cirrus cloud ice particles (Kärcher and Lohmann, 2002); (c) update to Sander et al. (2011) recommendations for cross sections of species, and the parameterisation of Minschwaner et al. (1993) for the Schumann–Runge bands, based on fixed-temperature opacity distribution function formulation; (d) upgrade of the radiative transfer code for calculations of photolysis, solar heating rates and top-of-atmosphere radiative forcing. The oceanic surface temperature is assimilated from the Hadley Centre for Climatic Prediction and Research; the parameterisation of periodic natural forcings (solar cycle, quasi-biennial oscillation) is included on-line.

The chemistry module (Pitari et al., 2002) is organised with long-lived and surface-flux species CH_4, N_2O, CFCs, HCFCs, CO, NMVOC, NO_x) and with all medium and short-lived species grouped in the families O_x, NO_y, HO_x, CHO_x, Cl_y, Br_y, SO_x and aerosols. In total there are 40 transported species and 26 species at photochemical equilibrium. For aerosols there are 57 size categories. The model includes the major components of stratospheric and tropospheric aerosols (sulphate, carbonaceous, soil dust, sea salt, PSCs). Aircraft NO_x emissions are emitted as the NO_x family species, and partitioned by applying photochemical equilibria between nitrogen species.

The updated radiative transfer module operating on-line in the ULAQ-CCM, is a two-stream delta-Eddington approximation model (Toon et al., 1989). It is used for chemical species photolysis rate calculations in ultra-violet (UV) to visible (VIS) wavelengths and for solar heating rates and radiative forcing in UV-VIS-near-infrared bands. The ULAQ model calculations of photolysis rates and surface and top-of-atmosphere radiative fluxes have been validated in the framework of SPARC and AEROCOM inter-comparison campaigns (Chipperfield et al., 2013; Randles et al., 2013).

2.4. Oslo CTM3

The Oslo CTM3 (Søvde et al., 2012) is a three dimensional off-line CTM. It is a recent upgrade of Oslo CTM2 (see Section 2.5). The improvements from Oslo CTM2 to CTM3 includes improved transport scheme parameterisation, wet scavenging processes, lightning parameterisation and calculations of photodissociation rates, as described by Søvde et al. (2012). The model is driven by 3-h forecasts generated by the Integrated Forecast System (IFS) of the ECMWF, cycle 36r1. Horizontal resolution is T42, and vertically the model domain spans 60 layers between the surface and 0.1 hPa. Vertical resolution is 700–900 m at aircraft cruise altitudes.

How the forecast data are put together is explained by Søvde et al. (2012). Advection of chemical species is carried out using the improved second order moments scheme (Prather et al., 2008; Søvde et al., 2012). Convective transport of tracers is based on the convective upward flux from the ECMWF model, allowing for entrainment or detrainment of tracers depending on the changes in the upward flux. Detrainment rates are read from the meteorological data, possibly increasing or decreasing the mixing with ambient air as the plume rises (Søvde et al., 2012). Turbulent mixing in the boundary layer is treated according to the Holtslag K-profile scheme (Holtslag et al., 1990).

Oslo CTM3 comprises comprehensive tropospheric chemistry, accounting for the most important parts of the O_3–NO_x–hydrocarbon chemistry cycle (Berntsen and Isaksen, 1997), the tropospheric sulphur cycle (Berglen et al., 2004), and also comprehensive stratospheric chemistry as explained in Søvde et al. (2008). Also included are tropospheric nitrate aerosols and sea salt aerosols. For the chemistry calculations, the quasi steady state approximation (QSSA) chemistry solver (Hesstvedt et al., 1978) is used.

Surface emissions are taken from RETRO (RETRO Emissions, 2006), except for biomass burning, which is taken from the Global Fires Emission Database version 3 (GFEDv3). Due to a conversion error, the Oslo CTM3 (and Oslo CTM2) assumed GFEDv3 NO_x to be NO_2 instead of NO, giving about 3 Tg (N) yr^{-1} instead of the correct 4.7 Tg (N) yr^{-1}. We have not had the possibility to re-run the simulations with correct value, but assume increasing surface NO_x emissions by 3–4% will not change the impact of aircraft emissions noticeably. Emissions of NO_x from lightning is described by Søvde et al. (2012), where the emissions are distributed through the year based on the amount of convection in the meteorological data.

2.5. Oslo CTM2

The Oslo CTM2 (Søvde et al., 2008) is the previous version of Oslo CTM3. It is widely used in previous studies (e.g. Berntsen and Isaksen, 1997; Berglen et al., 2004; Isaksen et al., 2005; Søvde et al., 2007, 2011). The chemistry schemes in Oslo CTM2 and Oslo CTM3 are the same; tropospheric and stratospheric chemistry is included, as is the tropospheric sulphur scheme. Due to computational constraints, CTM2 does not include tropospheric nitrate aerosols and sea salt aerosols in this study. The model resolution is the same as for CTM3, as are the meteorological data used to drive the model.

Compared to CTM3, the CTM2 advection of chemical species is calculated by the older second-order moment method (Prather, 1986). Convective transport is similar to CTM3, but does not use detrainment rates from meteorological data, thus having a somewhat more effective transport to higher altitudes (Søvde et al., 2012). Turbulent mixing is treated as in CTM3; according to the Holtslag K-profile scheme (Holtslag et al., 1990).

Surface emissions are the same as for CTM3. NO_x emissions from lightning differ from CTM3, and are coupled on-line to the

convection in the model using the parameterisation proposed by Price et al. (1997), along with their seasonal variation, as described by Berntsen and Isaksen (1999). In this work, we have updated the vertical distribution of lightning NO_x emissions to be the same as in Oslo CTM3. The old treatment often placed lightning NO_x at too high altitudes, even into the stratosphere. Effectively, the new treatment reduces UTLS NO_x, giving larger impact of the aircraft NO_x emissions. This update is further discussed in SM Sect. S3.

3. Aircraft emissions

REACT4C aircraft emissions inventories are produced using the FAST global aircraft movements and emissions model, one of the models approved for use by the International Civil Aviation Organization (ICAO)'s Committee on Aviation Environmental Protection (CAEP) Modelling and Database Group (MDG) (ICAO, 2013). FAST has been previously used in various applications such as the impacts of emissions trends (Lee et al., 2009; Owen et al., 2010; Olsen et al., 2013) and NO_x impacts on atmospheric chemistry (Gauss et al., 2006; Skowron et al., 2013).

The base case inventory is generated from 6 weeks of flight movements data from the year 2006, derived for the CAEP Round 8 (CAEP/8) MDG work programme (ICAO/CAEP, 2009), and found to be representative when extrapolated to an annual basis. Movement data are compiled from radar data of North American and European airspace, which covers ~80% of global civil aviation traffic. The remaining movements from the rest of the world are obtained from the Official Airline Guide (OAG). All flights were assumed to follow great circle trajectories, but with distance (and consequently fuel) correction applied using an empirical formula derived during the CAEP/8 Goals Modeling Work (ICAO/CAEP, 2009). This great circle correction is used to estimate actual distance and fuel burnt. The aircraft emissions are modelled using 42 aircraft types representative of the 2006 global fleet.

Annually averaged inventories are provided on a $1^\circ \times 1^\circ$ horizontal spacing and 610 m vertical spacing (2000 ft, one flight level), assuming standard atmosphere conditions. The latitude-height and horizontal distributions are shown in SM Fig. SF1.

Two possible mitigation inventories are produced, shifting cruise altitudes up and down 2000 ft, respectively, for aircraft types contributing >1% to the base case global fuel and distance flown (21 aircraft types). Fig. 1 shows global numbers of fuel (top) and NO_x (bottom) for each vertical level of the inventories. While distance flown is approximately 38.9 billion km in all inventories, fuel use is 178.3, 176.9 and 180.7 Tg yr^{-1} in bases case, +2000 ft and −2000 ft, respectively. For NO_x the corresponding numbers are 0.710, 0.716 and 0.710 Tg (N) yr^{-1}. The respective increase (1.3%) and decrease (0.8%) in fuel burnt observed for upward and downward shifts are to be expected, as generally the fuel efficiency increases with higher altitude. The opposite decrease (0.01%) and increase (0.8%) in NO_x emissions occur due to a higher NO_x emission index (EI) at higher altitudes, while a downward shift to a lesser extent reduces EI(NO_x).

4. Chemical impact

Before assessing the impact of the mitigation inventories, we quantify the overall chemical responses of aircraft NO_x emissions by comparing the base case simulations (BASE, BC for short) to simulations without aircraft emissions (NOAIR, NA). The mitigation option of flying higher (PLUS, PL) and lower (MINUS, MI) are then compared to BASE. Radiative forcing is discussed in Section 5.

Several studies have estimated the effect of aircraft NO_x emissions in the past, as summarised by Holmes et al. (2011). Both 5% perturbations (e.g. Hoor et al., 2009; Hodnebrog et al., 2012) and 100% perturbations (e.g., Gauss et al., 2006) have been applied. The latter gives the overall effect of aircraft, without considering compensating effects from other emission sectors due to chemical non-linearity (Grewe et al., 2010): A change in one NO_x emission

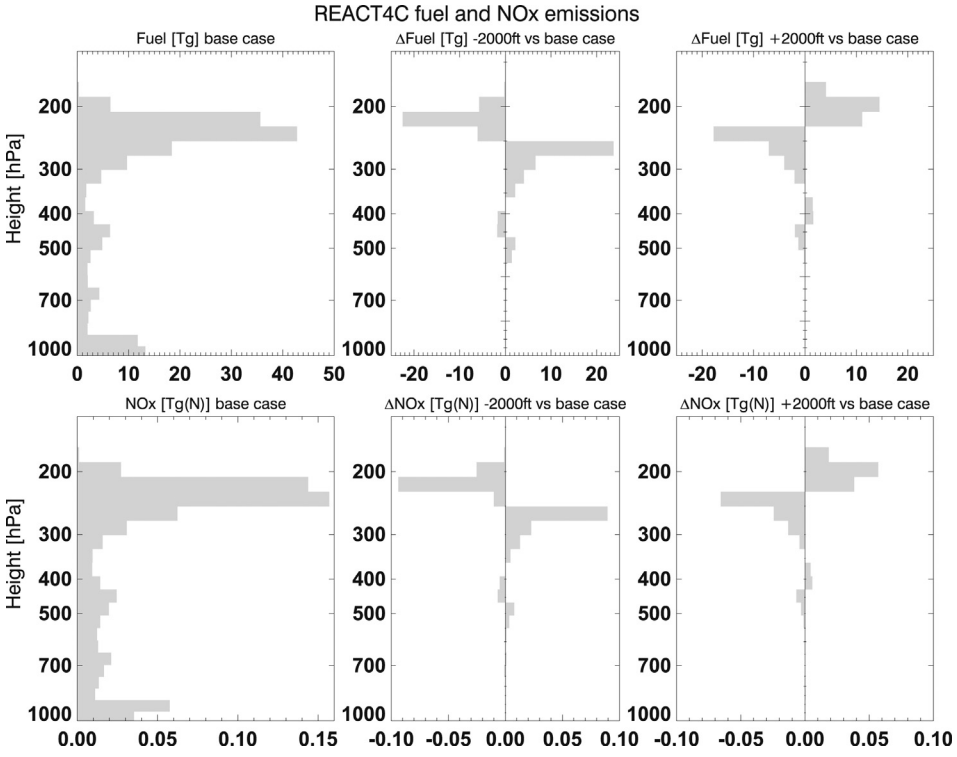

Fig. 1. Global annual emissions (Tg) of fuel (top) and NO_x (as atomic N, bottom), for all emission inventory levels.

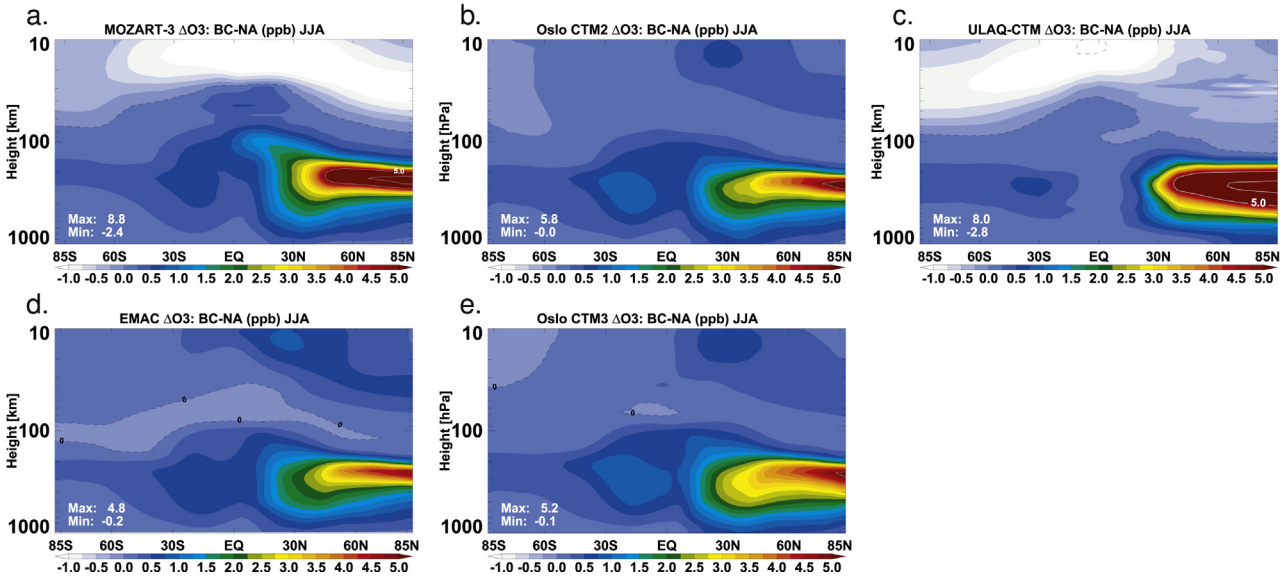

Fig. 2. Change in O_3 (ppb) due to aircraft emissions, calculated as the difference between the BASE minus NOAIR simulations for all models, for the JJA season. a. MOZART-3, b. Oslo CTM2, c, ULAQ-CTM, d. EMAC-QCTM and e. Oslo CTM3. White contours are 5 ppb and 7.5 ppb.

source (e.g. road traffic) may alter the effect on O_3 caused by another source (e.g. industrial emissions). For aircraft emissions, a possible compensating NO_x source could be lightning, and to assess how O_3 changes induced by lightning NO_x are modified by aircraft emissions, a tagging method has to be applied (Grewe et al., 2010; Grewe, 2013). Non-linear chemistry depends on the background of NO_x and hydrocarbons (Grewe et al., 2002; Köhler et al., 2008), but is often assumed to increase with larger changes in NO_x. Changing the geographic location may contribute to larger non-linearities (Köhler et al., 2008; Stevenson and Derwent, 2009). Grewe et al. (2002) found that aircraft NO_x produces O_3 more efficiently at lower altitudes, but is counterweighted by a shorter NO_x lifetime due to increased wet removal of HNO_3. Our vertical PLUS/MINUS inventories do not change the geographical emission patterns significantly, suggesting their non-linear impact will be relatively small. Non-linear effects in winter are expected to be smaller due to less sunlight. A thorough assessment of the non-linear chemistry following a vertical shift in cruise altitudes has been outside the scope of this work. Our main focus is to identify mitigation possibilities of flying higher or lower, so we apply the 100% perturbation method also for the comparison of BASE against NOAIR, even though this may mask non-linearities.

Generally, NO_x contributes to production of O_3 in the troposphere and to destruction of O_3 in the stratosphere (e.g. Grewe et al., 2002). Because of different transport schemes in the models, the amount of NO_x transported to the stratosphere will differ. We will come back to this in the next sections.

A change in NO_x sets up a perturbation in OH which again changes the greenhouse gas CH_4. For a NO_x increase, OH generally also increases, thereby reducing CH_4, whose main loss channel is through OH. A CH_4 perturbation has a long atmospheric lifetime (~12 years) and sets up a perturbation in O_3 having the same lifetime, usually referred to as the primary mode O_3. These long-lived changes in CH_4 and O_3 have the same sign. However, our model runs do not capture the long-lived changes in CH_4 and O_3, because we use fixed concentrations of CH_4 at the model surface. This is a well-known approach to reach chemical steady-state more quickly because the other species have shorter lifetimes than CH_4. While the method does not represent the "true" chemical steady-state because the long-lived effects of a CH_4 perturbation are missing, the method is still applicable because the radiative effects of CH_4 and the primary mode O_3 can be easily calculated from CH_4 lifetime changes. As will be explained in Section 5, this means that CH_4 can be allowed to differ slightly between the models.

To match the inventory year, the models also apply meteorological conditions for the year 2006, either driven directly (MOZART-3, Oslo CTM2, Oslo CTM3) or nudged (EMAC QCTM) by ECMWF meteorology, or as in ULAQ-CTM by using its own GCM winds. A month-by-month comparison may thus be less representative, so we present Jun-Jul-Aug (JJA) and Dec-Jan-Feb (DJF) seasonal averages for all models.

4.1. Base case aircraft NO_x emissions

Comparing BASE−NOAIR simulations we show the JJA zonal mean impact on O_3 from all models (Fig. 2), where maximum impact range from 4.8 ppb to 8.8 ppb. Winter time (DJF, Fig. 3) impact is smaller due to less photochemical activity, ranging from 3.4 ppb to 4.4 ppb. These impacts are consistent with earlier results (e.g., Hoor et al., 2009). Four features stand out in Figs. 2 and 3, namely an upper stratosphere reduction in MOZART-3 and ULAQ-CTM; larger vertical extent of the JJA ΔO_3 response in ULAQ-CTM; low DJF impact on O_3 at high latitudes in ULAQ-CTM; and a positive ΔO_3 at ~20 hPa in Oslo CTM2, EMAC-QCTM and Oslo CTM3. MOZART-3 and ULAQ-CTM seem to transport aircraft NO_x to higher altitudes (SM Figs. SF2 and SF3), increasing upper stratospheric O_3 destruction through the catalytic NO_x cycle. Next, the larger vertical extent of ΔO_3 in ULAQ-CTM is also seen for ΔNO_x and ΔNO_y (SM Figs. SF4 and SF5), indicating more vigorous vertical transport in extra-tropic cruise altitude regions. MOZART-3 has the highest ΔO_3, and although being more confined in the vertical at high latitudes, low-latitude ΔO_3 reach higher altitudes, suggesting faster upward transport in the tropics. The small DJF high latitude ΔO_3 in ULAQ-CTM can be explained by little photochemical activity and more effective downward transport, or possibly by a strong polar stratospheric vortex. Finally, the Oslo CTM2, EMAC-QCTM and Oslo CTM3 increase in O_3 at ~20 hPa is caused by reduced back-scattering of UV; more UV is absorbed at cruise altitudes. This is masked by the stratospheric NO_x increase in the other models.

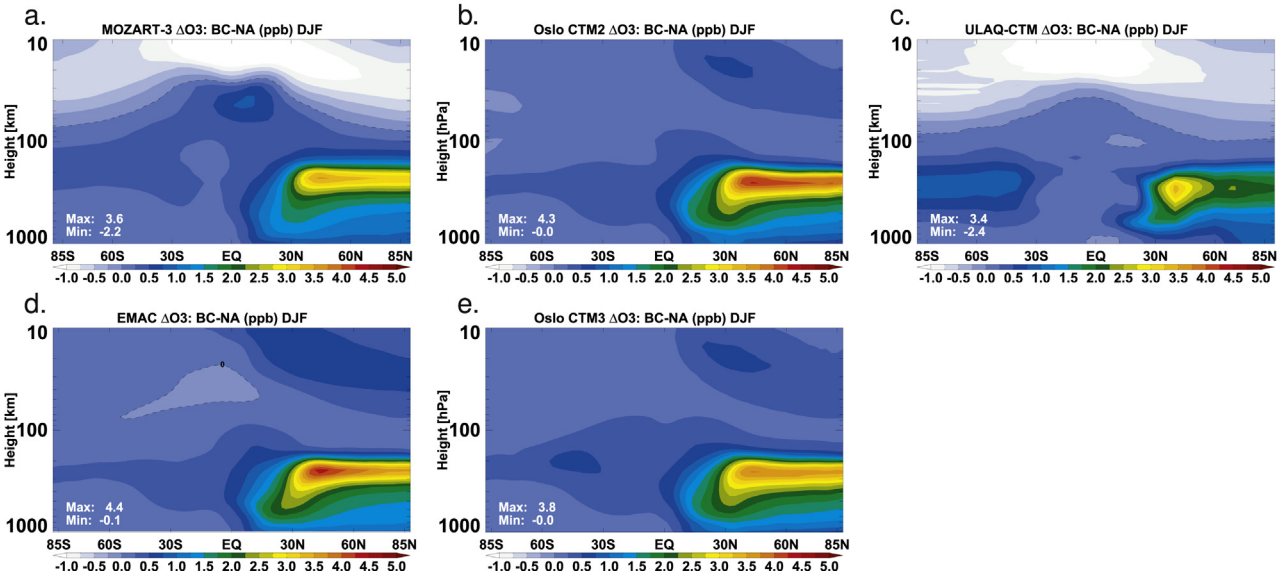

Fig. 3. Change in O_3 (ppb) due to aircraft emissions, calculated as the difference between the BASE minus NOAIR simulations for all models, for the DJF season.

Except for being transported to high altitudes in MOZART-3 and ULAQ-CTM, the modelled $NO_x = NO + NO_2$ is largely consistent between the models, with JJA maxima of about 47–64 ppb, except ULAQ-CTM which has about twice this value. In winter the models agree better on maximum values (56–70 ppb), which is shifted to mid-latitudes due to lack of sunlight at high latitudes. In general, the models agree on tropospheric NO_x and the inter-hemispheric transport. Similar features are found in NO_y and all non-HNO_3 nitrogen species (SM Figs. SF4–SF7). Larger impacts are accompanied by higher background values of NO_x and NO_y (SM Figs. SF10–SF17), indicating slower removal of atmospheric NO_y in ULAQ-CTM than in the other models. Higher background NO_x could also result in a smaller O_3 production efficiency.

Model differences in O_3 are thus mainly due to differences in transport or wet scavenging of NO_x or O_3 itself. These processes are important for determining the background distributions. The transport differences between the models should be sorted out in the future; it has unfortunately been out of scope of this work. Oslo CTM2 has typically lower background NO_x than Oslo CTM3, thereby having a larger impact of aircraft NO_x on O_3 (SM Figs. SF10–SF12 and Figs. SF14–SF16). Such changes are e.g. due to less wet removal of HNO_3, or slightly higher winter time NO_x emissions from lightning (Søvde et al., 2012), and should be expected to differ in the other models also.

All models except ULAQ-CTM have the largest impact on NO_x and NO_y in winter when aircraft at high latitudes fly more frequently in the stratosphere due to a lower tropopause, and hence the aircraft emissions are less subject to tropospheric wet removal. The reverse seasonal cycle in ULAQ-CTM is probably due to more removal of HNO_3 on ice cirrus during winter, but less wet scavenging during summer.

4.2. Plus 2000 ft aircraft NO_x emissions

The O_3 impact of increasing cruise altitude by 2000 ft is shown in Figs. 4 and 5, for JJA and DJF, respectively. In the region of maximum impact, i.e. 30°N–90°N at ~200 hPa, the JJA ΔO_3 is about 2 ppb compared to the BASE case. DJF ΔO_3 is expectedly smaller due to reduced photochemical activity, giving increases of up to 0.4–1.2 ppb compared to BASE. Otherwise, DJF and JJA show similar features. Oslo CTM2 and Oslo CTM3 have the largest winter time impact on ΔO_3, probably due to the lower background NO_x giving more effective O_3 production.

Compared to BASE, all models show O_3 reductions at higher stratospheric altitudes, with largest impacts for the models having largest stratospheric impact in BASE–NOAIR. An upward shift of cruise altitude reduces tropospheric NO_x, and thus slightly O_3. This reduction is largest in ULAQ-CTM where it also stretches equatorwards. Oslo CTM2 and CTM3, however, have no visible tropospheric reduction in the JJA zonal mean. On average, our models show an O_3 column increase of ~0.03 DU, consistent with previous studies (Gauss et al., 2006; Frömming et al., 2012). An increase is also consistent with Köhler et al. (2008).

In the region of maximum aircraft impact, a dipole structure can be seen in ULAQ-CTM (30°N, 275 hPa, Fig. 4), showing up more clearly in ΔNO_x and $\Delta(NO_y - HNO_3)$ (SM Figs. SF18–SF21). The ΔNO_x dipole is also seen in MOZART-3 and EMAC QCTM in JJA and in all models in DJF. The winter time dipole structures show up more clearly because more emissions are emitted in the stratosphere where the stable air acts to keep the sharp gradients in the vertical. This also applies for the mentioned dipole structures for O_3. Although the dipole is tilted differently in ULAQ-CTM, all models are generally consistent when it comes to changes in reactive nitrogen species.

Cruise region NOx changes vary from −4% to ~10% in summer and −10% to ~30% in winter (SM Figs. SF24–SF25), suggesting that non-linearities play a small role in summer but may be important in winter. We also note that the small winter ΔNO_y in ULAQ-CTM (SM Figs. SF23 and SF5) is probably due to more efficient HNO_3 loss on cirrus ice in winter.

4.3. Minus 2000 ft aircraft emissions

Lowering the cruise altitude by 2000 ft reduces the impact on O_3 (Figs. 6 and 7). In the region of maximum impact, summer time ΔO_3 is reduced by up to 1–2 ppb compared to the BASE case. This reduction is smaller in winter due to less photochemical activity.

In general, this response is almost opposite of PLUS–BASE. The models show an increase in upper-stratospheric O_3, most pronounced in the models where BASE–NOAIR has the strongest stratospheric impact. A slight increase in O_3 in the lower

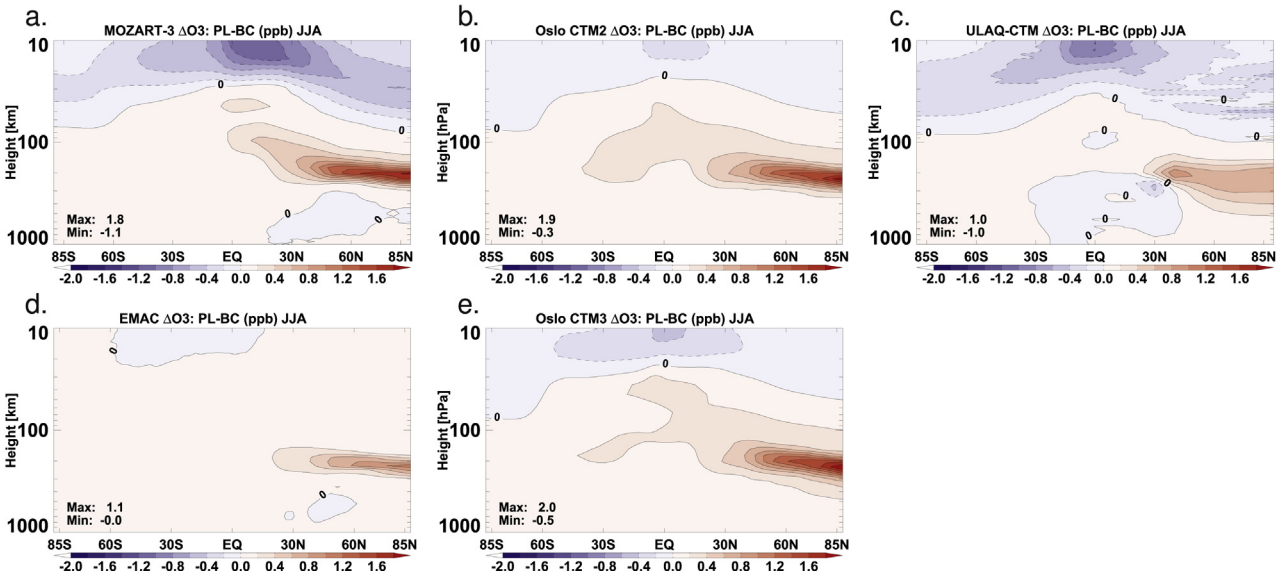

Fig. 4. Change in O_3 (ppb) due to lifting aircraft emissions by 2000 ft, calculated as the difference between the PLUS minus BASE simulations, for the JJA season. Contours are shown for every 0.2 ppb.

troposphere is seen, least pronounced in Oslo CTM3. The total O_3 column is reduced by ~0.02 DU, consistent with previous studies (Gauss et al., 2006; Köhler et al., 2008; Frömming et al., 2012), Corresponding ΔNO_x, $\Delta(NO_y - HNO_3)$ and ΔNO_y are shown in the SM Figs. SF26–SF33; largely showing opposite features compared to PLUS–BASE.

5. Radiative forcing estimates

Short-lived O_3 radiative forcings (RFs) have been calculated for all simulations performed in this study, using two different radiative transfer models (RTM) in off-line simulations, namely the Oslo and ULAQ radiative models. We discuss these results before describing the CH_4 related forcing.

The Oslo RTM uses separate radiative transfer codes for long-wave and short-wave radiation (Myhre et al., 2011), more specifically a broad band code (Myhre and Stordal, 1997) and the multi-stream DISORT code (Stamnes et al., 1988), respectively. Stratospheric temperature adjustment is included in the simulations, to follow the standard definition of radiative forcing (Forster et al., 2007). See SM Sect. S4 for more details.

The ULAQ radiative transfer module is the same as used in the ULAQ-CCM (Section 2.3), and has been validated in the framework of SPARC and AEROCOM inter-comparison campaigns (Chipperfield et al., 2013; Randles et al., 2013). It applies a two-stream delta-Eddington approximation model in the solar spectrum (Randles et al., 2013), and a two-stream delta-Eddington broad band correlated-k distribution model in the long-wave planetary spectrum (Chou et al., 2000). Stratospheric temperature adjustment is performed in the Fixed Dynamic Heating (FDH) approximation (Ramanathan and Dickinson, 1979). See SM Sect. S4 for more details.

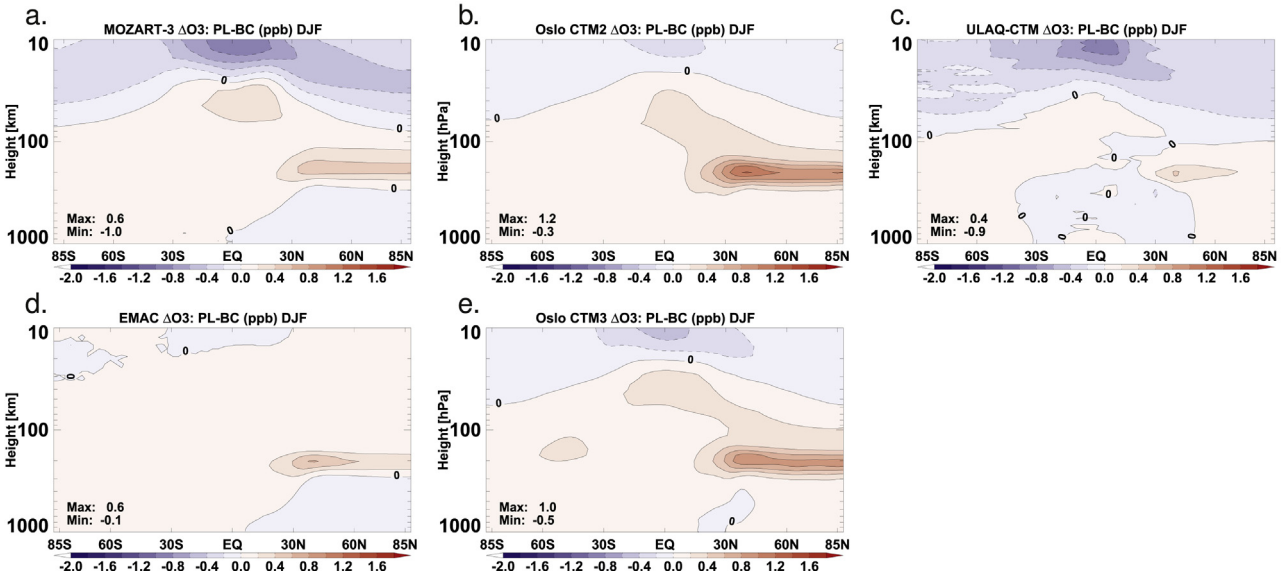

Fig. 5. Change in O_3 (ppb) due to lifting aircraft emissions by 2000 ft, calculated as the difference between the PLUS minus BASE simulations, for the DJF season. Contours are shown for every 0.2 ppb.

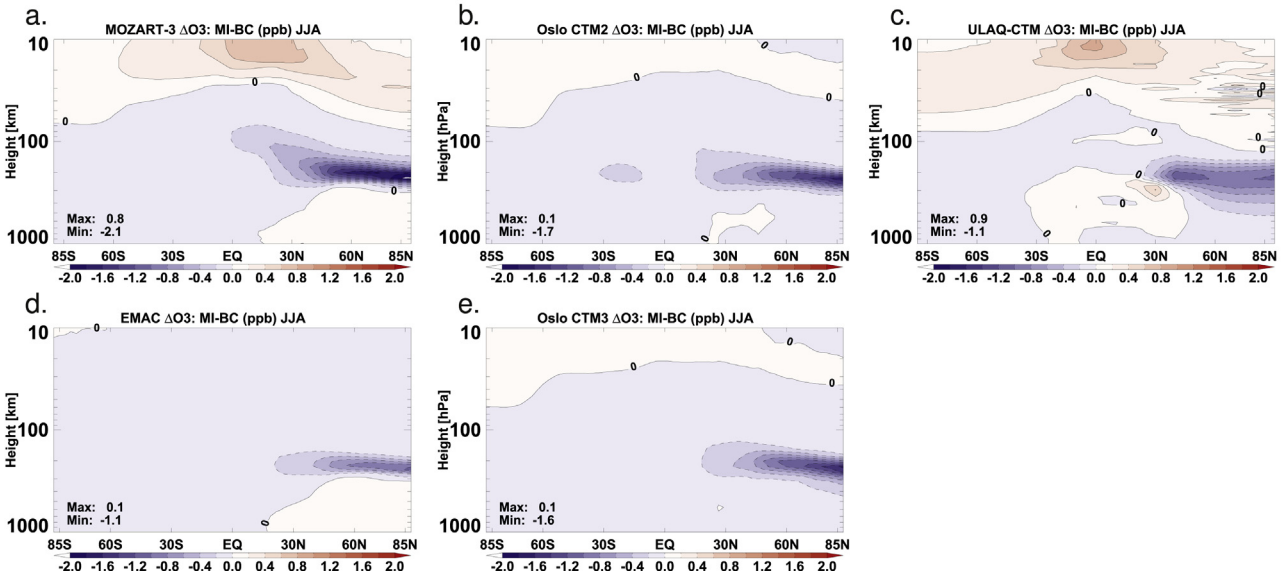

Fig. 6. Change in O_3 (ppb) due to lowering aircraft emissions by 2000 ft, calculated as the difference between the MINUS minus BASE simulations, for the JJA season. Contours are shown for every 0.2 ppb.

Annual RFs for short-lived O_3 are listed in Table 1 for all model runs, separated into short wave forcing (SW), long wave forcing adjusted for stratospheric temperature change (LW) and net forcing (Net), showing that the two RTMs agree fairly well, especially for LW. For the BASE−NOAIR, our models produce net annual RF ranging from 16.4 mW m^{-2} to 23.5 mW m^{-2}, with a mean of ~19.5 mW m^{-2}. MOZART-3 has the smallest RF due to the smallest SW contribution, even though its LW forcing is slightly higher than for ULAQ-CTM. Oslo CTM2 and CTM3 have higher RFs, and differ internally by about 1.3 mW m^{-2}, mainly caused by LW. Net RF between the RTMs differs by about 0–5%, while LW about 5–15% and SW 15–20%. This is in line with Stevenson et al. (2013).

Annual mean RF differences between the models mainly originate during winter time, while in summer the models agree better (SM Sect. S5). Noticeable lower winter time RFs in ULAQ-CTM and partly in MOZART-3 correspond well with their smaller tropical O_3 perturbations in the zonal means, and can also be seen in the horizontal RF distribution (SM Sect. S5). This strengthens the indication that ULAQ-CTM and to some extent MOZART-3 have stronger tropical upwelling than the other models. We also note that relative differences in monthly O_3 RF between the RTMs are similar to their annual mean differences.

Scaling to 1 Tg (N) yr^{-1} emissions, we find the short-lived O_3 RF from aircraft to be 27.4 mW m^{-2}, comparing well with the 27.3 ± 9.7 mW m^{-2} of Holmes et al. (2011). Our results are somewhat higher than the QUANTIFY studies (Myhre et al., 2011; Hodnebrog et al., 2012) giving ~21 mW m^{-2}, i.e. we have a higher sensitivity per emission. However, because of the differences in spatial and temporal distribution of REACT4C and QUANTIFY emissions, such a direct comparison should be carried out with care (Skowron et al., 2013).

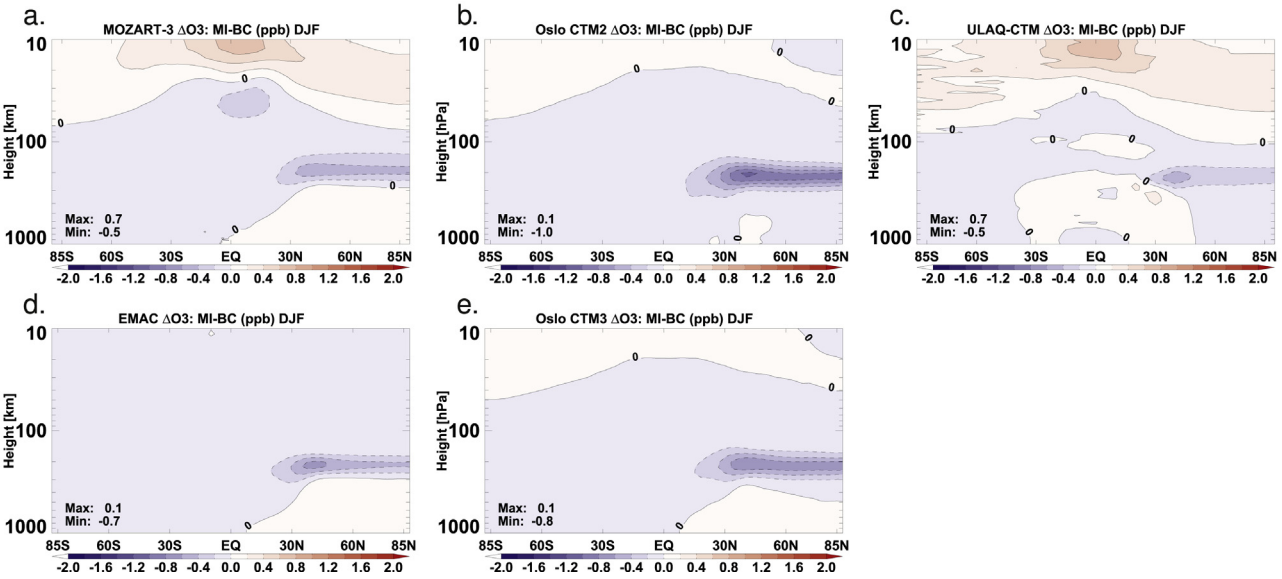

Fig. 7. Change in O_3 (ppb) due to lowering aircraft emissions by 2000 ft, calculated as the difference between the MINUS minus BASE simulations, for the DJF season. Contours are shown for every 0.2 ppb.

Table 1
Short-lived O_3 radiative forcing for the different models, using the Oslo and ULAQ radiative models. Units are mW m^{-2}. LW is adjusted for stratospheric change in temperature, hence Net is also adjusted.

Model	RF calc.					
	BASE–NOAIR					
	SW		LW		Net	
	OSLO	ULAQ	OSLO	ULAQ	OSLO	ULAQ
MOZART-3	3.52	3.04	12.9	13.5	16.4	16.6
ULAQ-CTM	4.93	4.24	12.5	13.3	17.4	17.5
EMAC QCTM	4.51	3.88	14.0	15.8	18.5	19.7
Oslo CTM2	4.74	3.97	16.4	18.3	21.1	22.2
Oslo CTM3	5.28	4.43	17.1	19.0	22.4	23.5
	PLUS–BASE					
MOZART-3	0.03	0.08	1.18	1.14	1.20	1.22
ULAQ-CTM	0.17	0.13	0.34	0.33	0.51	0.46
EMAC QCTM	0.05	0.00	0.90	0.90	0.95	0.90
Oslo CTM2	0.19	0.12	2.75	2.72	2.94	2.84
Oslo CTM3	0.13	0.07	2.28	2.24	2.41	2.30
	MINUS–BASE					
MOZART-3	0.03	0.00	−1.13	−1.07	−1.11	−1.04
ULAQ-CTM	−0.15	−0.12	−0.45	−0.32	−0.59	−0.44
EMAC QCTM	−0.03	−0.09	−0.86	−0.79	−0.89	−0.89
Oslo CTM2	−0.21	−0.17	−2.22	−2.23	−2.43	−2.40
Oslo CTM3	−0.15	−0.23	−1.75	−1.74	−1.89	−1.97

A 2000 ft higher cruise altitude produces a small RF increase ranging from about 0.5 mW m^{-2} to 2.9 mW m^{-2}, with smallest impact in ULAQ-CTM and largest in Oslo CTM2. The largest changes are caused by increased LW, most pronounced during summer months, and the amount of RF largely follows the ΔO_3 in Figs. 4 and 5. Thus the RF differences are related to the differences in transport and background NO_x between the models; emitting more often in the stratosphere, the compensating negative RF at high altitudes is increased.

Flying at altitudes 2000 ft lower consistently changes the sign of LW RF, although absolute values are similar to PLUS vs BASE. A change in sign is also seen for SW RF, except for MOZART-3 where SW RF is zero or slightly positive. The largest contribution to forcing changes is still from LW, and the net RF ranges from about −0.5 to −2.4 mW m^{-2}, compared to the BASE case. As for the PLUS case, CTM2 produces the largest change, closely followed by CTM3. Roughly halving their values, we find the RF from MOZART-3 and EMAC QCTM, and about another halving we get the RF from ULAQ-CTM. The downward shift of aircraft NO_x emissions reduces upper-stratospheric O_3 destruction, and also puts a larger fraction of the emissions into the troposphere. Not only is tropospheric NO_x removed more quickly through rainout of HNO_3, the downward shift of ΔO_3 also acts to reduce the forcing.

Based on CH_4 lifetime changes, we calculate the RF from CH_4 as in IPCC (2001) and Myhre et al. (2011), using a specific forcing of 0.37 mW m^{-2} ppb^{-1} together with a background CH_4 concentration of 1740 ppb. The latter is assumed to change proportionally to fractional change in CH_4 lifetime, hence a RF can be calculated even if the model CH_4 concentrations differ slightly. However, all models have tropospheric CH_4 concentrations close to this number, around 1760 ppb. The CH_4 lifetimes due to loss to OH are listed in Table 2, along with changes due to different aircraft emission inventories, all calculated from modelled monthly means of OH, CH_4 and temperature. We find that BASE−NOAIR produce an RF for CH_4 ranging from −10.7 mW m^{-2} to −7.1 mW m^{-2} (Table 3). Increasing cruise altitudes leads to 0–0.2 mW m^{-2} increase in this RF, while decreasing cruise altitudes decrease it by 0.1–0.4 mW m^{-2}. Long-lived ΔO_3 caused by changes in CH_4 are calculated according to IPCC AR5 (Myhre et al., 2013), i.e. as 50% of the CH_4 RF. CH_4 changes

Table 2
CH_4 lifetime due to loss to OH (years), for NOAIR (NA) and absolute differences for the different model simulations. Not corrected for feedback factor.

Model	NA	BC−NA	PL−BC	MI−BC
MOZART-3	8.544	−0.068	0.0020	−0.0040
ULAQ-CTM	8.390	−0.067	0.0012	−0.0019
EMAC QCTM	9.822	−0.117	0.0016	−0.0025
Oslo CTM2	9.646	−0.096	0.0010	−0.0010
Oslo CTM3	8.344	−0.087	≈0	−0.0010

will change stratospheric water vapour and give an additional RF of 15% of CH_4 RF (Myhre et al., 2007).

The total annual RFs due to our 0.71 Tg (N) yr^{-1} aircraft NO_x emissions are listed in Table 4, giving mean RF of ~5 mW m^{-2}, with a range of 1–8 mW m^{-2}. Cruising at the 2000 ft higher altitude increases this RF by about 2 ± 1 mW m^{-2}, while cruising at the 2000 ft lower altitude reduces it by 2 ± 1 mW m^{-2}.

6. Summary and conclusions

This work comprises a multi-model assessment of the aircraft NO_x emission impact on the atmosphere for the contrail-avoiding mitigation possibilities of shifting the main cruise altitudes up or down one flight level. Updated aircraft emission inventories based on year 2006 aircraft movements have been applied, and the models comprise comprehensive tropospheric and stratospheric chemistry to fully cover the UTLS.

The chemical O_3 perturbation and sensitivity to the altitude of aircraft NO*x* emissions are consistent with earlier studies (e.g., Gauss et al., 2006; Köhler et al., 2008; Frömming et al., 2012).

We find the short-lived O_3 changes due to 0.71 Tg (N) yr^{-1} of aircraft NO_x emissions to cause an RF of 19 ± 3 mW m^{-2}, or 27 ± 5 mW m^{-2} when scaled to 1 Tg (N) yr^{-1}, matching Holmes et al. (2011) well. Our RF from CH_4 is in the lower range of Holmes et al. (2011), while RF from primary mode O_3 is somewhat higher due to new IPCC recommendations; previously the RF of the primary mode was estimated to be about 30% of the CH_4 RF, but has now been updated to 50% (Myhre et al., 2013).

Accounting for CH_4 related changes we find a total RF due to aircraft NO_x of about 5 mW m^{-2}, with a range of 1–8 mW m^{-2}. The lower end of this range is due to one model giving a stronger effect on CH_4, and without this model the range would be about 4–8 mW m^{-2}, with a mean of 6 mW m^{-2}.

Shifting cruise altitudes, and hence aircraft NO_x emissions, 2000 ft upwards increases the total RF due to gaseous photochemistry by about 2 ± 1 mW m^{-2}. Similarly, a downward shift of 2000 ft reduces the RF by about 2 ± 1 mW m^{-2}. Scaled to 1 Tg (N) yr^{-1}, this amounts to about 2.5 ± 1.5 mW m^{-2}. These changes are mainly driven by short-lived O_3, of which they represent about 10%.

Table 3
RF (mW m^{-2}) from changes in CH_4 lifetime in Table 2, adjusted for feedback factor, and the long-lived changes of O_3 and stratospheric H_2O, calculated as explained in the text.

Model	BC−NA	PL−BC	MI−BC
	RF CH_4		
MOZART-3	−7.117	0.211	−0.422
ULAQ-CTM	−7.198	0.130	−0.206
EMAC QCTM	−10.733	0.152	−0.234
Oslo CTM2	−8.970	0.094	−0.094
Oslo CTM3	−9.398	0.000	−0.109
	RF long-lived O_3 = 0.5 RF(CH_4)		
	RF stratospheric H_2O = 0.15 RF(CH_4)		

Table 4
Total changes in RF (mW m^{-2}) from short-lived O_3, long-lived O_3, CH_4 and the increase of stratospheric H_2O due to CH_4 changes. To include the range of RF for short-lived O_3 from both RTMs, two numbers are listed for each entry.

Model	BC–NA	PL BC	MI–BC
MOZART-3	4.65/4.81	1.55/1.57	−1.80/−1.73
ULAQ-CTM	5.32/5.52	0.75/0.77	−0.92/−0.80
EMAC QCTM	0.83/1.99	1.20/1.15	−1.27/−1.27
Oslo CTM2	6.30/7.43	3.09/2.99	−2.59/−2.55
Oslo CTM3	6.88/7.95	2.41/2.30	−2.07/−1.97
Mean	5.2	1.8	−1.8

We have not assessed the potential of aircraft aerosol emissions to affect the radiative budget. Aerosols may absorb or scatter light, and also have an impact on NO_x by providing surfaces for conversion to HNO_3. The latter effect is small and reduces the aircraft-induced O_3 by ~10% (Iachetti et al., 2014, personal communication, in preparation).

Burkhardt and Kärcher (2011) found AIC RF to be about 31 mW m^{-2}, and Myhre et al. (2013) suggest 50 mW m^{-2}. While Frömming et al. (2012) and Fichter et al. (2005) studied cruise altitude shifts and found linear contrail RF changes smaller or comparable to RF of short-lived O_3, the linear contrail RF is only about 10% of total contrail cirrus RF (Burkhardt and Kärcher, 2011). Thus, the potential for AIC RF changes is larger; if it can be reduced substantially by flying higher or lower, the accompanying NO_x-related RF will be small. As explained in Section 3, the long-lived CO_2 will also be affected by a vertical cruise altitude shift. However, comparing RFs with very different lifetimes requires a choice of emission scenario and also a time horizon. Lee et al. (2010) found the historically accumulated RF(CO_2) to be 28 mW m^{-2}, which is of the order of the short-lived O_3 instantaneous RF, meaning that eventually CO_2 will control the total aviation climate impact. Our vertical shifts in cruise altitudes change aircraft CO_2 emissions by less than 1%, and using specific RF from Myhre et al. (2013) the following changes in instantaneous annual RF(CO_2) are about 0.01 mW m^{-2} yr^{-1}, which is small compared to the NO_x and AIC RFs. Assuming sustained aircraft emissions, the consequential change in surface temperature when flying higher or lower will mainly be caused by NO_x and AIC, even after 100 years. We stress, however, that CO_2 is still important for the total climate impact of aircraft.

A contrail study could in principle be set up for our inventories, but this has been outside the scope of our work. Also, there are very few models calculating aerosol and cirrus effects; building a multi-model comparison for these would increase the confidence in their results.

Acknowledgements

This work was carried out within the EU project REACT4C, grant number ACP8-GA-2009-233772. We acknowledge Emily Gray for starting the work on MOZART-3.

Appendix A. Supplementary data

Supplementary data related to this article can be found at http://dx.doi.org/10.1016/j.atmosenv.2014.06.049.

References

Berglen, T.F., Berntsen, T.K., Isaksen, I.S.A., Sundet, J.K., 2004. A global model of the coupled sulfur/oxidant chemistry in the troposphere: the sulfur cycle. J. Geophys. Res. 109 (D19310), D19310. http://dx.doi.org/10.1029/2003JD003948.

Berntsen, T., Fuglestvedt, J., Myhre, G., Stordal, F., Berglen, T.F., 2006. Abatement of greenhouse gases: does location matter? Clim. Change 74 (4), 377–411. http://dx.doi.org/10.1007/s10584-006-0433-4.

Berntsen, T., Isaksen, I.S.A., 1997. A global 3-D chemical transport model for the troposphere, 1, Model description and CO and Ozone results. J. Geophys. Res. 102 (D17), 21239–21280. http://dx.doi.org/10.1029/97JD01140.

Berntsen, T.K., Isaksen, I.S.A., 1999. Effects of lightning and convection on changes in upper tropospheric ozone due to NOx emissions from aircraft. Tellus 51B, 766–788. http://dx.doi.org/10.1034/j.1600-0889.1999.t01-3-00003.x.

Burkhardt, U., Kärcher, B., 2011. Global radiative forcing from contrail cirrus. Nat. Clim. Change 1, 54–58. http://dx.doi.org/10.1038/nclimate1068.

Chipperfield, M., Liang, Q., Bekki, S., Douglass, A., Kinnison, D., Plummer, D., Prather, M., Sinnhuber, B., 2013. Sparc Report No. 6: Lifetimes of Stratospheric Ozone-depleting Substances, Their Replacements, and Related Species, Chapter 5: Model Estimates of Lifetimes. www.sparc-climate.org/publications/sparc-reports/sparc-report-no6/.

Chou, M.-D., Suarez, M.J., Liang, X.-Z., Yan, M.M.-H., 2000. Technical Report Series on Global Modeling and Data Assimilation, NASA/TM-2001-104606. A Thermal Infrared Radiation Parameterization for Atmospheric Studies, vol. 19.

Dameris, M., Grewe, V., Köhler, I., Sausen, R., Brühl, C., Grooß, J.-U., Steil, B., 1998. Impact of aircraft NOx emissions on tropospheric and stratospheric ozone. Part II: 3-D model results. Atmos. Environ. 32 (18), 3185–3199. http://dx.doi.org/10.1016/S1352-2310(97)00505-0.

Deckert, R., Jöckel, P., Grewe, V., Gottschaldt, K.-D., Hoor, P., 2011. A quasi chemistry-transport model mode for EMAC. Geosci. Model Dev. 4 (1), 195–206. http://dx.doi.org/10.5194/gmd-4-195-2011.

Eyring, V., Butchart, N., Waugh, D.W., Akiyoshi, H., Austin, J., Bekki, S., Bodeker, G.E., Boville, B.A., Br"uhl, C., Chipperfield, M.P., Cordero, E., Dameris, M., Deushi, M., Fioletov, V.E., Frith, S.M., Garcia, R.R., Gettelman, A., Giorgetta, M.A., Grewe, V., Jourdain, L., Kinnison, D.E., Mancini, E., Manzini, E., Marchand, M., Marsh, D.R., Nagashima, T., Newman, P.A., Nielsen, J.E., Pawson, S., Pitari, G., Plummer, D.A., Rozanov, E., Schraner, M., Shepherd, T.G., Shibata, K., Stolarski, R.S., Struthers, H., Tian, W., Yoshiki, M., 2006. Assessment of temperature, trace species, and ozone in chemistry-climate model simulation of the recent past. J. Geophys. Res. 111, D22308. http://dx.doi.org/10.1029/2006JD007327.

Fichter, C., Marquart, S., Sausen, R., Lee, D.S., 2005. The impact of cruise altitude on contrails and related radiative forcing. Meteorol. Z. 14 (4), 563–572. http://dx.doi.org/10.1127/0941-2948/2005/0048.

Forster, P., Ramaswamy, V., Artaxo, P., Berntsen, T., Betts, R., Fahey, D., Haywood, J., Lean, J., Lowe, D., Myhre, G., Nganga, J., Prinn, R., Raga, G., Schulz, M., Van Dorland, R., 2007. Contribution of working group i to the fourth assessment report of the intergovernmental panel on climate change. In: Solomon, S., Qin, D., Manning, M., Chen, Z., Marquis, M., Averyt, K., Tignor, M., Miller, H. (Eds.), Climate Change 2007: the Physical Science Basis. Cambridge University Press, Cambridge, United Kingdom and New York, NY, USA.

Forster, P.F., Shine, K.P., 1997. Radiative forcing and temperature trends from stratospheric ozone changes. J. Geophys. Res. 102 (D9), 10841–10855. http://dx.doi.org/10.1029/96JD03510.

Frömming, C., Ponater, M., Dahlmann, K., Grewe, V., Lee, D.S., Sausen, R., 2012. Aviation-induced radiative forcing and surface temperature change in dependency of the emission altitude. J. Geophys. Res. 117 (D19), D19104. http://dx.doi.org/10.1029/2012JD018204.

Gauss, M., Isaksen, I.S.A., Lee, D.S., Søvde, O.A., 2006. Impact of aircraft NOx emissions on the atmosphere – tradeoffs to reduce the impact. Atmos. Chem. Phys. 6, 1529–1548. http://dx.doi.org/10.5194/acp-6-1529-2006.

Gettelman, A., Kinnison, D.E., Brasseur, G., Dunkerton, T., 2004. Impact of monsoon circulations on the upper troposphere and lower stratosphere. J. Geophys. Res. 109, D22101. http://dx.doi.org/10.1029/2004JD004878.

Granier, C., Lamarque, J.F., Mieville, A., Muller, J.F., Olivier, J., Orlando, J., Peters, J., Petron, G., Tyndall, G., Wallens, S., 2005. POET, A Database of Surface Emissions of Ozone Precursors. Available on internet at http://www.aero.jussieu.fr/projet/ACCENT/POET.php.

Grewe, V., 2013. A generalized tagging method. Geosci. Model Dev. 6 (1), 247–253. http://dx.doi.org/10.5194/gmd-6-247-2013.

Grewe, V., Brunner, D., Dameris, M., Grenfell, J.L., Hein, R., Shindell, D., Staehelin, J., 2001. Origin and variability of upper tropospheric nitrogen oxides and ozone at northern mid-latitudes. Atmos. Environ. 35 (20), 3421–3433. http://dx.doi.org/10.1016/S1352-2310(01)00134-0.

Grewe, V., Dameris, M., Fichter, C., Lee, D.S., 2002. Impact of aircraft NOx emissions. Part 2: effects of lowering the flight altitude. Meteorol. Z. 11 (3), 197–205. http://dx.doi.org/10.1127/0941-2948/2002/0011-0197.

Grewe, V., Stenke, A., Ponater, M., Sausen, R., Pitari, G., Iachetti, D., Rogers, H., Dessens, O., Pyle, J., Isaksen, I.S.A., Gulstad, L., Søvde, O.A., Marizy, C., Pascuillo, E., 2007. Climate impact of supersonic air traffic: an approach to optimize a potential future supersonic fleet – Results from the EU-project SCENIC. Atmos. Chem. Phys. 7, 5129–5145. http://dx.doi.org/10.5194/acp-7-5129-2007.

Grewe, V., Tsati, E., Hoor, P., 2010. On the attribution of contributions of atmospheric trace gases to emissions in atmospheric model applications. Geosci. Model Dev. 3 (2), 487–499. http://dx.doi.org/10.5194/gmd-3-487-2010.

Hack, J.J., 1994. Parameterization of moist convection in the NCAR community climate model (CCM2). J. Geophys. Res. 99 (D3), 5551–5568. http://dx.doi.org/10.1029/93JD03478.

Hansen, J., Sato, M., Ruedy, R., 1997. Radiative forcing and climate response. J. Geophys. Res. 102, 6831–6864. http://dx.doi.org/10.1029/96JD03436.

Hesstvedt, E., 1974. Reduction of stratospheric ozone from high-flying aircraft, studied in a two-dimensional photochemical model with transport. Can. J. Chem. 52 (8), 1592–1598. http://dx.doi.org/10.1139/v74-231.

Hesstvedt, E., Hov, Ö., Isaksen, I.S.A., 1978. Quasi steady-state approximation in air pollution modelling: comparison of two numerical schemes for oxidant prediction. Int. J. Chem. Kinetics X, 971–994. http://dx.doi.org/10.1002/kin.550100907.

Hidalgo, H., Crutzen, P.J., 1977. The tropospheric and stratospheric composition perturbed by NOx emissions of high-altitude aircraft. J. Geophys. Res. 82, 5833–5866. http://dx.doi.org/10.1029/JC082i037p05833.

Hodnebrog, Ø., Berntsen, T.K., Dessens, O., Gauss, M., Grewe, V., Isaksen, I.S.A., Koffi, B., Myhre, G., Olivié, D., Prather, M.J., Stordal, F., Szopa, S., Tang, Q., van Velthoven, P., Williams, J.E., 2012. Future impact of traffic emissions on atmospheric ozone and OH based on two scenarios. Atmos. Chem. Phys. 12 (24), 12211–12225. http://dx.doi.org/10.5194/acp-12-12211-2012.

Holmes, C.D., Tang, Q., Prather, M.J., 2011. Uncertainties in climate assessment for the case of aviation NO. Proc. Natl. Acad. Sci. 108 (27), 10997–11002. http://dx.doi.org/10.1073/pnas.1101458108.

Holtslag, A.A.M., DeBruijn, E.I.F., Pan, H.-L., 1990. A high resolution air mass transformation model for short-range weather forecasting. Mon. Wea. Rev. 118, 1561–1575. http://dx.doi.org/10.1175/1520-0493(1990)118<1561:AHRAMT>2.0.CO;2.

Hoor, P., Borken-Kleefeld, J., Caro, D., Dessens, O., Endresen, O., Gauss, M., Grewe, V., Hauglustaine, D., Isaksen, I.S.A., Jöckel, P., Lelieveld, J., Myhre, G., Meijer, E., Olivie, D., Prather, M., Poberaj, C.S., Shine, K.P., Staehelin, J., Tang, Q., van Aardenne, J., van Velthoven, P., Sausen, R., 2009. The impact of traffic emissions on atmospheric ozone and OH: results from QUANTIFY. Atmos. Chem. Phys. 9, 3113–3136. http://dx.doi.org/10.5194/acp-9-3113-2009.

ICAO, 2013. International Civil Aviation Organization. http://www.icao.int/environmental-protection/Pages/modelling-and-databases.aspx. last accessed (29.04.13.).

ICAO/CAEP, 2009. International Civil aviation Organization (ICAO)/Committee on Aviation Environmental Protection (CAEP), Agenda Item 4: Modeling and Databases Task Force (MODTF Goals Assessment Results. In: ICAO/CAEP Working Paper, Steering Group Meeting, Salvador, Brazil, 22–26 June 2009.

IPCC, 2001. Climate Change 2001: the Scientific Basis. Contribution of Working Group I to the Third Assessment Report of the Intergovernmental Panel on Climate Change. Cambridge University Press, Cambridge, United Kingdom and New York, NY, USA, p. 881.

Isaksen, I.S.A., Zerefos, C., Kourtidis, K., Meleti, C., Dalsøren, S.B., Sundet, J.K., Grini, A., Zanis, P., Balis, D., 2005. Tropospheric ozone changes at unpolluted and semipolluted regions induced by stratospheric ozone changes. J. Geophys. Res. 110 (D2), D02302. http://dx.doi.org/10.1029/2004JD004618.

Jöckel, P., Kerkweg, A., Pozzer, A., Sander, R., Tost, H., Riede, H., Baumgaertner, A., Gromov, S., Kern, B., 2010. Development cycle 2 of the Modular Earth Submodel System (MESSY2). Geosci. Model Dev. 3 (2), 717–752. http://dx.doi.org/10.5194/gmd-3-717-2010.

Jöckel, P., Tost, H., Pozzer, A., Brühl, C., Buchholz, J., Ganzeveld, L., Hoor, P., Kerkweg, A., Lawrence, M., Sander, R., Steil, B., Stiller, G., Tanarhte, M., Taraborrelli, D., van Aardenne, J., Lelieveld, J., 2006. The atmospheric chemistry general circulation model ECHAM5/MESSY1: consistent simulation of ozone from the surface to the mesosphere. Atmos. Chem. Phys. 6 (12), 5067–5104. http://dx.doi.org/10.5194/acp-6-5067-2006.

Johnson, C., Henshaw, J., McInnes, G., 1992. Impact of aircraft and surface emissions of nitrogen oxides on tropospheric ozone and global warming. Nature 355 (6355), 69–71. http://dx.doi.org/10.1038/355069a0.

Johnston, H.S., 1971. Reduction of stratospheric ozone by nitrogen oxide catalysts from supersonic transport exhaust. Science 173, 517–522. http://dx.doi.org/10.1126/science.173.3996.517.

Kärcher, B., Lohmann, U., 2002. A parameterization of cirrus cloud formation: homogeneous freezing of supercooled aerosols. J. Geophys. Res. 107, 4010,. http://dx.doi.org/10.1029/2001JD000470.

Kerkweg, A., 2005. Global Modelling of Atmospheric Halogen Chemistry in the Marine Boundary Layer. Ph.D. Thesis. University of Bonn, Germany. Available at: http://hss.ulb.uni-bonn.de/2005/0636/0636.htm.

Kinnison, D.E., Brausser, G.P., Walters, S., Garcia, R.R., Marsh, D.R., Sassi, F., Harvey, V.L., Randall, C.E., Emmons, L., Lamarque, J.F., Hess, P., Orlando, J.J., Tie, X.X., Randel, W., Pan, L.L., Gettelman, A., Granier, C., Diehl, T., Niemeier, U., Simmons, A.J., 2007. Sensitivity of chemical tracers to meteorological parameters in the MOZART-3 chemical transport model. J. Geophys. Res. 112, D20302. http://dx.doi.org/10.1029/2006JD007879.

Köhler, M.O., Rädel, G., Dessens, O., Shine, K.P., Rogers, H.L., Wild, O., Pyle, J.A., 2008. Impact of perturbations to nitrogen oxide emissions from global aviation. J. Geophys. Res. 113 (D11), D11305,. http://dx.doi.org/10.1029/2007JD009140.

Köhler, M.O., Rädel, G., Shine, K.P., Rogers, H.L., Pyle, J.A., 2013. Latitudinal variation of the effect of aviation NOx emissions on atmospheric ozone and methane and related climate metrics. Atmos. Environ. 64, 1–9. http://dx.doi.org/10.1016/j.atmosenv.2012.09.013.

Lacis, A.A., Wuebbles, D.J., Logan, J.A., 1990. Radiative forcing of climate by changes in the vertical-distribution of ozone. J. Geophys. Res. 95, 9971–9981. http://dx.doi.org/10.1029/JD095iD07p09971.

Lamarque, J.-F., Bond, T.C., Eyring, V., Granier, C., Heil, A., Klimont, Z., Lee, D., Liousse, C., Mieville, A., Owen, B., Schultz, M.G., Shindell, D., Smith, S.J., Stehfest, E., Van Aardenne, J., Cooper, O.R., Kainuma, M., Mahowald, N., McConnell, J.R., Naik, V., Riahi, K., van Vuuren, D.P., 2010. Historical (1850–2000) gridded anthropogenic and biomass burning emissions of reactive gases and aerosols: methodology and application. Atmos. Chem. Phys. 10 (15), 7017–7039. http://dx.doi.org/10.5194/acp-10-7017-2010.

Lee, D.S., Fahey, D.W., Forster, P.M., Newton, P.J., Wit, R.C.N., Lim, L.L., Owen, B., Sausen, R., 2009. Aviation and global climate change in the 21st century. Atmos. Environ. 43 (34), 3520–3537. http://dx.doi.org/10.1016/j.atmosenv.2009.04.024.

Lee, D.S., Pitari, G., Grewe, V., Gierens, K., Penner, J.E., Petzold, A., Prather, M.J., Schumann, U., Bais, A., Berntsen, T., Iachetti, D., Lim, L.L., Sausen, R., 2010. Transport impacts on atmosphere and climate: Aviation. Atmos. Environ. 44 (37), 4678–4734. http://dx.doi.org/10.1016/j.atmosenv.2009.06.005.

Lin, S.J., Rood, R.B., 1996. A fast flux form semi-lagrangian transport scheme on the sphere. Mon. Weather Rev. 124, 2046–2070. http://dx.doi.org/10.1175/1520-0493(1996)124<2046:MFFSLT>2.0.CO;2.

Liu, Y., Liu, C.X., Wang, H.P., Tie, X.X., Gao, S.T., Kinnison, D., Brasseur, G., 2009. Atmospheric tracers during the 2003–2004 stratospheric warming event and impact of ozone intrusions in the troposphere. Atmos. Chem. Phys. 9, 2157–2170. http://dx.doi.org/10.5194/acp-9-2157-2009.

Lohmann, U., Roeckner, E., 1996. Design and performance of a new cloud microphysics scheme developed for the ECHAM general circulation model. Clim. Dynam. 12, 557–572. http://dx.doi.org/10.1007/BF00207939.

Minschwaner, K., Salawitch, R.J., McElroy, M.B., 1993. Absorption of solar radiation by O_2: implications for O_3 and lifetimes of N_2O, $CFCl_3$, and CF_2Cl_2. J. Geophys. Res. 98, 10543–10561. http://dx.doi.org/10.1029/93JD00223.

Morgenstern, O., Giorgetta, M.A., Shibata, K., Eyring, V., Waugh, D.W., Shepherd, T.G., Akiyoshi, H., Austin, J., Baumgaertner, A.J.G., Bekki, S., Braesicke, P., Brühl, C., Chipperfield, M.P., Cugnet, D., Dameris, M., Dhomse, S., Frith, S.M., Garny, H., Gettelman, A., Hardiman, S.C., Hegglin, M.I., Jöckel, P., Kinnison, D.E., Lamarque, J.-F., Mancini, E., Manzini, E., Marchand, M., Michou, M., Nakamura, T., Nielsen, J.E., Olivié, D., Pitari, G., Plummer, D.A., Rozanov, E., Scinocca, J.F., Smale, D., Teyssèdre, H., Toohey, M., Tian, W., Yamashita, Y., 2010. Review of the formulation of present-generation stratospheric chemistry-climate models and associated external forcings. J. Geophys. Res. 115, D00M02. http://dx.doi.org/10.1029/2009JD013728.

Myhre, G., Nilsen, J.S., Gulstad, L., Shine, K.P., Rognerud, B., Isaksen, I.S.A., 2007. Radiative forcing due to stratospheric water vapour from CH4 oxidation. Geophys. Res. Lett. 34, L01807. http://dx.doi.org/10.1029/2006GL027472.

Myhre, G., Shindell, D., Bréon, F.-M., Collins, W., Fuglestvedt, J., Huang, J., Koch, D., Lamarque, J.-F., Lee, D., Mendoza, B., Nakajima, T., Robock, A., Stephens, G., Takemura, T., Zhang, H., 2013. Anthropogenic and natural radiative forcing. Climate Change 2013: the Physical Science Basis. Contribution of Working Group I to the Fifth Assessment Report of the Intergovernmental Panel on Climate Change. Cambridge University Press, Cambridge, United Kingdom and New York, NY, USA.

Myhre, G., Shine, K., Rädel, G., Gauss, M., Isaksen, I., Tang, Q., Prather, M., Williams, J., van Velthoven, P., Dessens, O., Koffi, B., Szopa, S., Hoor, P., Grewe, V., Borken-Kleefeld, J., Berntsen, T., Fuglestvedt, J., 2011. Radiative forcing due to changes in ozone and methane caused by the transport sector. Atmos. Environ. 45 (2), 387–394. http://dx.doi.org/10.1016/j.atmosenv.2010.10.001.

Myhre, G., Stordal, F., 1997. Role of spatial and temporal variations in the computation of radiative forcing and GWP. J. Geophys. Res. 102 (D10), 11181–11200. http://dx.doi.org/10.1029/97JD00148.

Olsen, S.C., Wuebbles, D.J., Owen, B., 2013. Comparison of global 3-D aviation emissions datasets. Atmos. Chem. Phys. 13, 429–442. http://dx.doi.org/10.5194/acp-13-429-2013.

Owen, B., Lee, D.S., Lim, L., 2010. Flying into the Future: Aviation Emissions Scenarios to 2050. Environ. Sci. Technol. 44 (7), 2255–2260. http://dx.doi.org/10.1021/es902530z.

Park, M., Randel, W.R., Kinnison, D.E., Garcia, R.R., Choi, W., 2004. Seasonal variations of methane, water vapor, ozone, and nitrogen dioxide near the tropopause: Satellite observations and model simulations. J. Geophys. Res. 109, D03302. http://dx.doi.org/10.1029/2003JD003706.

Pickering, K.E., Wang, Y.S., Tao, W.K., Price, C., Muller, J.F., 1998. Vertical distributions of lightning NOx for use in regional and global chemical transport models. J. Geophys. Res. 103 (D23), 31203–31216. http://dx.doi.org/10.1029/98JD02651.

Pitari, G., Iachetti, D., Mancini, E., Montanaro, V., Marizy, C., Dessens, O., Rogers, H., Pyle, J., Grewe, V., Stenke, A., Søvde, O.A., 2008. Radiative forcing from particle emissions by future supersonic aircraft. Atmos. Chem. Phys. 8, 4069–4084. http://dx.doi.org/10.5194/acp-8-4069-2008.

Pitari, G., Mancini, E., Rizi, V., Shindell, D.T., 2002. Impact of Future Climate and Emission Changes on Stratospheric Aerosols and Ozone. J. Atmos. Sci. 59, 414–440. http://dx.doi.org/10.1175/1520-0469(2002)059<0414:IOFCAE>2.0.CO;2.

Prather, M.J., 1986. Numerical advection by conservation of second-order moments. J. Geophys. Res. 91 (D6), 6671–6681. http://dx.doi.org/10.1029/JD091iD06p06671.

Prather, M.J., Zhu, X., Strahan, S.E., Steenrod, S.D., Rodriguez, J.M., 2008. Quantifying errors in trace species transport modeling. Proc. Natl. Acad. Sci. USA 105 (50), 19617–19621. http://dx.doi.org/10.1073/pnas.0806541106.

Price, C., Penner, J., Prather, M., 1997. NOx from lightning 1. Global distribution based on lightning physics. J. Geophys. Res. 102 (D5), 5929–5941. http://dx.doi.org/10.1029/96JD03504.

Ramanathan, V., Dickinson, R., 1979. The role of stratospheric ozone in the zonal and seasonal radiative energy balance of the earth-troposphere system. J. Atmos. Sci. 36 (6), 1084–1104.

Randles, C.A., Kinne, S., Myhre, G., Schulz, M., Stier, P., Fischer, J., Doppler, L., Highwood, E., Ryder, C., Harris, B., Huttunen, J., Ma, Y., Pinker, R.T., Mayer, B., Neubauer, D., Hitzenberger, R., Oreopoulos, L., Lee, D., Pitari, G., Genova, G.D., Rose, F.G., Kato, S., Rumbold, S.T., Vardavas, I., Hatzianastassiou, N., Matsoukas, C., Yu, H., Zhang, F., Zhang, H., Lu, P., 2013. Intercomparison of shortwave radiative transfer schemes in global aerosol modeling: results from the AeroCom Radiative Transfer Experiment. Atmos. Chem. Phys. 13, 2347–2379. http://dx.doi.org/10.5194/acp-13-2347-2013.

Rasch, P.J., Mahowald, N.M., Eaton, B.E., 1997. Representations of transport, convection, and the hydrological cycle in chemical transport models: Implications for the modeling of short-lived and soluble species. J. Geophys. Res. 102 (D23), 28127–28138. http://dx.doi.org/10.1029/97JD02084.

RETRO Emissions, 2006. Reanalysis of the Tropospheric Chemical Composition Over the Past 40 years. http://retro.enes.org/.

Roeckner, E., Bäuml, G., Bonaventura, L., Brokopf, R., Esch, M., Giorgetta, M., Hagemann, S., Kirchner, I., Kornblueh, L., Manzini, E., Rhodin, A., Schlese, U., Schulzweida, U., Tompkins, A., 2003. The atmospheric general circulation model ECHAM5. Part I: Model description. Rep./MPI Fr. Meteorol. 349. Max Planck Institute for Meteorology, http://pubman.mpdl.mpg.de/pubman/item/escidoc:995269:2/component/escidoc:995268/Report-349.pdf.

Roeckner, E., Brokopf, R., Esch, M., Giorgetta, M., Hagemann, S., Kornblueh, L., Manzini, E., Schlese, U., Schulzweida, U., 2006. Sensitivity of simulated climate to horizontal and vertical resolution in the ECHAM5 Atmosphere Model. J. Clim. 19 (16), 3771–3791. http://dx.doi.org/10.1175/JCLI3824.1.

Sander, R., Kerkweg, A., Jöckel, P., Lelieveld, J., 2005. Technical note: the new comprehensive atmospheric chemistry module mecca. Atmos. Chem. Phys. 5, 445–450. http://dx.doi.org/10.5194/acp-5-445-2005.

Sander, S.P., Abbatt, J., Barker, J.R., Burkholder, J.B., Friedl, R.R., Golden, D.M., Huie, R.E., Kolb, C.E., Kurylo, M.J., Moortgat, G.K., Orkin, V.L., Wine, P.H., 2011. Chemical Kinetics and Photochemical Data for Use in Atmospheric Studies. Evaluation No. 17. Tech. Rep. 10-06. Jet Propulsion Laboratory, Pasadena. California Institute of Technology. http://jpldataeval.jpl.nasa.gov/.

Sander, S.P., Finlayson-Pitts, B.J., Friedl, R.R., Golden, D.M., Huie, R.E., Keller-Rudek, H., Kolb, C.E., Kurylo, M.J., Molina, M.J., Moortgat, G.K., Orkin, V.L., Ravishankara, A.R., Wine, P.H., 2006. Chemical Kinetics and Photochemical Data for Use in Atmospheric Studies. Evaluation No. 15. Tech. Rep. 06-2. Jet Propulsion Laboratory, Pasadena. California Institute of Technology. http://jpldataeval.jpl.nasa.gov/.

Sassi, F., Kinnison, D.E., Boville, B.A., Garcia, R.R., Roble, R., 2004. Effect of El Niño – Southern Oscillation on the dynamical, thermal, and chemical structure of the middle atmosphere. J. Geophys. Res. 109, D17108. http://dx.doi.org/10.1029/2003JD004434.

Schumann, U., 1997. The impact of nitrogen oxides emissions from aircraft upon the atmosphere at flight altitudes – results from the aeronox project. Atmos. Environ. 31 (12), 1723–1733. http://dx.doi.org/10.1016/S1352-2310(96)00326-3.

Skowron, A., Lee, D.S., de León, R.R., 2013. The assessment of the impact of aviation NOx on ozone and other radiative forcing responses – The importance of representing cruise altitudes accurately. Atmos. Environ. 74, 159–168. http://dx.doi.org/10.1016/j.atmosenv.2013.03.034.

Søvde, O.A., Gauss, M., Isaksen, I.S.A., Pitari, G., Marizy, C., 2007. Aircraft pollution – A futuristic view. Atmos. Chem. Phys. 7, 3621–3632. http://dx.doi.org/10.5194/acp-7-3621-2007.

Søvde, O.A., Gauss, M., Smyshlyaev, S.P., Isaksen, I.S.A., 2008. Evaluation of the chemical transport model Oslo CTM2 with focus on Arctic winter ozone depletion. J. Geophys. Res. 113 (D09304), D09304. http://dx.doi.org/10.1029/2007jd009240.

Søvde, O.A., Hoyle, C.R., Myhre, G., Isaksen, I.S.A., 2011. The HNO_3 forming branch of the HO_2+ NO reaction: pre-industrial-to-present trends in atmospheric species and radiative forcings. Atmos. Chem. Phys. 11 (17), 8929–8943. http://dx.doi.org/10.5194/acp-11-8929-2011.

Søvde, O.A., Prather, M.J., Isaksen, I.S.A., Berntsen, T.K., Stordal, F., Zhu, X., Holmes, C.D., Hsu, J., 2012. The chemical transport model Oslo CTM3. Geosci. Model Dev. 5, 1441–1469. http://dx.doi.org/10.5194/gmd-5-1441-2012.

Stamnes, K., Tsay, S., Wiscombe, W., Jayaweera, K., 1988. Numerically stable algorithm for discrete-ordinate-method radiative transfer in multiple scattering and emitting layered media. Appl. Opt. 27 (12), 2502–2509. http://dx.doi.org/10.1364/AO.27.002502.

Stevenson, D.S., Derwent, R.G., 2009. Does the location of aircraft nitrogen oxide emissions affect their climate impact? Geophys. Res. Lett. 36, L17810. http://dx.doi.org/10.1029/2009GL039422.

Stevenson, D.S., Young, P.J., Naik, V., Lamarque, J.-F., Shindell, D.T., Voulgarakis, A., Skeie, R.B., Dalsren, S.B., Myhre, G., Berntsen, T.K., Folberth, G.A., Rumbold, S.T., Collins, W.J., MacKenzie, I.A., Doherty, R.M., Zeng, G., van Noije, T.P.C., Strunk, A., Bergmann, D., Cameron-Smith, P., Plummer, D.A., Strode, S.A., Horowitz, L., Lee, Y., Szopa, S., Sudo, K., Nagashima, T., Josse, B., Cionni, I., Righi, M., Eyring, V., Conley, A., Bowman, K.W., Wild, O., Archibald, A., 2013. Tropospheric ozone changes, radiative forcing and attribution to emissions in the Atmospheric Chemistry and Climate Model Inter-comparison Project (ACCMIP). Atmos. Chem. Phys. 13, 3063–3085. http://dx.doi.org/10.5194/acp-13-3063-2013.

Stordal, F., Gauss, M., Myhre, G., Mancini, E., Hauglustaine, D.A., Köhler, M.O., Berntsen, T., Stordal, E.J.G., Iachetti, D., Pitari, G., Isaksen, I.S.A., 2006. Tradeoffs in climate effects through aircraft routing: forcing due to radiatively active gases. Atmos. Chem. Phys. Discuss. 6, 10733–10771. http://dx.doi.org/10.5194/acpd-6-10733-2006.

Sundqvist, H., 1978. A parameterization scheme for non-convective condensation including prediction of cloud water content. Q. J. Roy. Meteor. Soc. 104, 677–690. http://dx.doi.org/10.1002/qj.49710444110.

Tanré, D., Geleyn, J.-F., Slingo, J.M., 1984. First results of the introduction of an advanced aerosol-radiation interaction in the ECMWF low resolution global model. In: Gerber, H., Deepak, A. (Eds.), Aerosols and Their Climatic Effects. A. Deepak Publ., Hampton, VA, pp. 133–177.

Toon, O.B., McKay, C.P., Ackerman, T.P., Santhanam, K., 1989. Rapid calculation of radiative heating rates and photodissociation rates in inhomogeneous multiple scattering atmospheres. J. Geophys. Res. 94, 16287–16301. http://dx.doi.org/10.1029/JD094iD13p16287.

Wang, W.C., Sze, N.D., 1980. Coupled effects of atmospheric N_2O and O_3 on the earth's climate. Nature 286, 589–590. http://dx.doi.org/10.1038/286589a0.

Wuebbles, D.J., Patten, K.O., Wang, D., Youn, D., Martnez-Aviles, M., Francisco, J.S., 2011. Three-dimensional model evaluation of the Ozone Depletion Potentials for n-propyl bromide, trichloroethylene and perchloroethylene. Atmos. Chem. Phys. 11, 2371–2380. http://dx.doi.org/10.5194/acp-11-2371-2011.

Yi, B., Yang, P., Liou, K.-N., Minnis, P., Penner, J.E., 2012. Simulation of the global contrail radiative forcing: a sensitivity analysis. Geophys. Res. Lett. 39 (24), 28. http://dx.doi.org/10.1029/2012GL054042.

Zhang, G.J., McFarlane, N.A., 1995. Sensitivity of climate simulations to the parameterization of cumulus convection in the Canadian climate centre general circulation model. Atmos. Ocean. 33 (3), 407–446. http://dx.doi.org/10.1080/07055900.1995.9649539.